

Date of publication xxxx 00, 0000, date of current version xxxx 00, 0000.

Digital Object Identifier 10.1109/ACCESS.2017.DOI

A New Three-Phase Multi-level Asymmetrical Inverter with Optimum Hardware Components

DHANAMJAYULU C^{1,2}, (Member, IEEE), PALANISAMY K^{1,2}, (Senior, IEEE), SANJEEVIKUMAR PADMANABAN², (SENIOR MEMBER, IEEE), PANDAV KIRAN MAROTI², (Member, IEEE), AND JENS BO HOLM-NIELSEN², (Senior Member, IEEE)

¹School of Electrical Engineering, Vellore Institute of Technology, Vellore, Tamil Nadu, India

²Department of Energy Technology, Aalborg University, Esbjerg, Denmark

Corresponding author: Dhanamjayulu C (e-mail: dhanamjayulu.c@vit.ac.in) and Sanjeevikumar Padmanaban (e-mail: san@et.aau.dk).

“This project is carried out under the Project No. 19-MG06AAU, Danida Mobility Grant, responsible for the Ministry of Foreign Affairs of Denmark (MFA), Act 7 on Denmark’s International Development Cooperation.”

ABSTRACT In this paper, a novel three-phase asymmetrical multilevel inverter is presented. The proposed inverter is designed with an optimal hardware components to generate three-phase nineteen output voltage levels. The proposed inverter exhibits various advantages like a suitable output voltage waveform with improved power quality, lower total harmonic distortion (THD), and more moderate complexity, reduction in cost, reduced power losses, and improved efficiency. A comparison of the proposed topology in terms of several parameters with existing methods illustrates its merits and features. The proposed inverter tested with steady-state and dynamic load disturbances. Various experimental results are included in this paper to validate the performance of the proposed inverter during various extremities. In addition, a detailed comparison is tabulated between simulation and experimental results graphically. The proposed inverter has been stable even during load disturbance conditions. The simulation and feasibility model are verified using a prototype model.

INDEX TERMS Multilevel Inverter(MLI), Total Harmonic Distortion, Asymmetrical Multilevel Inverter

I. INTRODUCTION

THE multilevel inverter is gaining a lot of importance in industrial and high-power applications because of the usage of low-level inverter results in an output with more significant harmonics. So, the research and study of these multilevel inverters are gaining a lot of importance. There are different methods to realize the working of multilevel inverters [1-6]. The most prominent among these topologies is neutral point clamped inverters, the flying capacitors, and the cascaded inverters [2]. These topologies are aided with different switching patterns like single pulse width modulation SPWM, multi-carrier pulse width modulation MCPWM, and staircase modulation technique to achieve AC output voltage waveform with lower harmonics. With an increased number of levels of the inverter, the THD improves. In a neutral point clamped method [7-9], diodes are used to facilitate multiple voltage levels to the capacitor bank connected in cascade mode via various phases. The diodes are the clamping devices that allow limited voltage to transfer through them,

reducing the stress from other devices. The peak voltage of these inverters is half of the energy supplied, which is one shortfall and the same can be eliminated by aggregating the number of diodes, switches, and condensers, the output voltage is limited and for over three-levels the charge balance gets disturbed. The applications of these inverters include static Var compensation, variable motor speed drives, high voltage DC and AC transmission lines, high voltage system inter-connection. Flying capacitors [10] topology is quite similar to the diode-clamped multilevel inverter, but capacitors clamping devices in this method, unlike the diode-clamped MLI [23-39].

In recent past, modular multilevel converters (MMC) are suited for high-voltage applications and these are introduced with various sub-modules, where each sub-module comprises two switches with a DC capacitor. The switching losses and harmonics are less. Number of switches and capacitors are used in this topology, which increases the control complexity and cost [11, 12]. There are three types of multilevel

inverters neutral point clamped (NPC) [13], Cascade H-bridge inverter (CHB) [14] and flying capacitor (FC) [15]. Number of switches and clamping diodes are used in diode-clamped inverter for higher levels, moreover the balancing of capacitors is a challenging task as these are connected in series. Even for higher levels, larger number of capacitors are used in flying capacitor where the balancing of voltage is complex [16].

The advantage of symmetric structures is modularity that can able to design and extend easily. Two such inverter structures are presented in [17, 18], where the mixture of basic units and H-bridge used based on non-isolated DC sources require number of switches, increases the control complexity, size and cost. A new multilevel inverter topology with insulated driver circuit and reduced number of switches has been presented in [19]. In addition, the calculation of DC voltage sources is proposed, and it comprises four high rating switches. This requires a bi-directional switch for the blocking voltage and conducting current in both directions.

In [20], a three-phase multilevel inverter suited for electrical drive applications has been presented. Counterpart of the CHB inverters, power cells are cascaded, and each cell is having two series legs. The design equations for the load voltage with steps carried out using pulse-width modulation phase shifting multi-carrier modulation technique are analyzed. There are several DC voltage sources in this topology results in the increase in the total cost of the inverter which is a disadvantage of this structure.

A new topology of multilevel inverter is presented in [21]. This structure mainly focuses on reducing the power transistors regarding the number of levels. Various equations are derived mathematically. This requires a bi-directional switch for the blocking voltage and conducting current in both directions.

This paper presents a reduced circuit part for renewable energy applications, counting inverter topology at nineteen levels. This manuscript presents a 19-level asymmetric cascaded MLI with reduced DC sources and switches with relatively low THD. The proposed inverter is implemented and tested only with a resistive, inductive load, and dynamic variations in the load from R to L and vice versa. The analysis of total standing voltage can be done [22]. During the dynamic load period conditions, the proposed inverter is well stabilized [23-41], and this inverter is suitable for renewable energy applications [23-41].

The article was structured as follows. Section II that follows contains the details of the proposed topology of 19-levels. Part III presents the parameter calculations, section IV presents the loss and efficiency, section V presents TSV calculation, and section VI and section VII present the findings of the analysis and experiment along with the simulation results.

II. PROPOSED THREE-PHASE ASYMMETRICAL INVERTER TOPOLOGY

The proposed three-phase 19-level-inverter is shown in Fig. 1. The topology proposed for each phase comprises two bidirectional and nine unidirectional power semiconductor switches for each phase leg is shown in Fig. 2. The bidirectional switches are used to avoid short-circuits and to block currents in both directions for the DC supply. In this topology, usually, the desired voltage is realized from different DC voltage links or sources. Based on the DC sources, the cascaded MLIs are classified as symmetrical (equal) and asymmetrical (unequal) inverters. In symmetrical type, the voltage of the DC links is held at the same level. The demerit of symmetrical topology is that with the increase in output voltage levels, the number of switches also increases. In order to overcome this, the DC links are supplied with unequal voltages called the asymmetrical topology. In the proposed 19 level asymmetrical MLI, the switches are selected based on the strategy in avoiding short circuit in the specified path of current traversal. The initial level is got by conducting the switches S_3 , S_5 , S_A , T_A and T_B forming a closed path precisely without short circuit. In this mode of operation, the blocking voltage of switches is in calculating the total standing voltage. In the second mode of operation, the switches S_2 , S_5 , S_A , T_A , T_B are in conduction. These are selected for avoiding the short circuit, and even the addition of maximum blocking voltages of each semiconductor switch is lesser in value, which results in less TSV and cost effective. Similarly, the switch selection patterns up to 19 level are represented in Table.3. Based on this look-up table, the switches are selected based on the above conditions in which the overall loop of conduction of switches provides an efficient operation of an inverter with less standing voltage across switches. The proposed topology is implemented with three unequal DC sources namely, $V_1=133.5$, $V_2=44.5V$, and $V_3=222.5V$ and load resistance 100 ohms, respectively. The switching losses in the system depend on switching frequency, which is less because of the reduced voltage. This topology also comprises the combining of various switches to enhance the efficiency of the inverter. The switching states for the proposed inverter are tabulated in Table I. The proposed inverter phase A and modes of operation are shown in Fig. 3 to 21, respectively. In Mode-1, the power switches S_3 , S_5 , S_A , T_A , and T_B are turn-on (conduction state) and remaining switches will turn-off then, the output voltage is the sum of $V_O=V_1+V_2+V_3=+400.5V$ at the load ends. In Mode-2, the power switches S_2 , S_5 , S_A , T_A , and T_B are turn-on (conduction state) and remaining switches will turn-off then, the output voltage is the sum of $V_O=V_1+V_3=+356V$ at the load ends. In Mode-3, the power switches S_2 , S_A , S_B , T_A , and T_B are turn-on (conduction state) and remaining switches will turn-off then, the output voltage is the sum of $V_O=V_1-V_2+V_3=+311.5V$ at the load ends. In Mode-4, the power switches S_1 , S_3 , S_5 , T_A , and T_B are turn-on (conduction state) and remaining switches will turn-off then, the output voltage is the sum of $V_O=V_2+V_3=+267V$ at

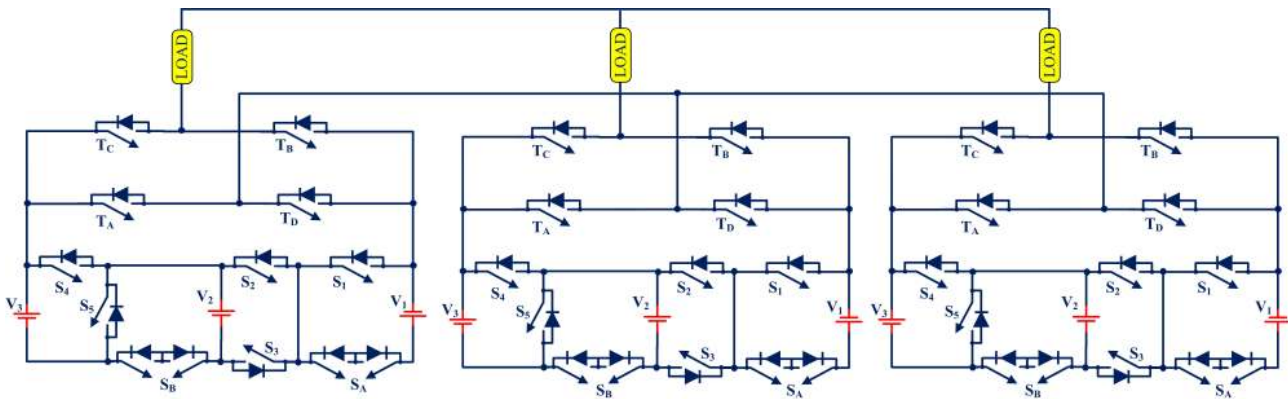


FIGURE 1. Proposed Three-Phase Configuration of 19MLI

the load ends. In Mode-5, the power switches $S_1, S_2, S_5, T_A,$ and T_B are turn-on (conduction state) and remaining switches will turn-off then, the output voltage is $V_O = V_3 = +222.5V$ at the load ends. In Mode-6, the power switches $S_3, S_4, S_A, T_A,$ and T_B are turn-on (conduction state) and remaining switches will turn-off then, the output voltage is the sum of $V_O = V_1 + V_2 = +178V$ at the load ends. In Mode-7, the power switches $S_2, S_4, S_A, T_A,$ and T_B are turn-on (conduction state) and remaining switches will turn-off then, the output voltage is $V_O = V_1 = +133.5V$ at the load ends. In Mode-8, the power switches $S_2, S_4, S_5, S_A, S_B, T_A,$ and T_B are turn-on (conduction state) and remaining switches will turn-off then, the output voltage is the sum of $V_O = V_1 - V_2 = 89V$ at the load ends. In Mode-9, the power switches $S_1, S_3, S_4, T_A,$ and T_B are turn-on (conduction state) and remaining switches will turn-off then, the output voltage is $V_O = V_2 = 44.5V$ at the load ends. In Mode-10, the power switches $T_B,$ and T_D are turn-on (conduction state) and remaining switches will turn-off then, the output voltage is $V_O = 0V$ at the load ends. In Mode-11, the power switches $S_1, S_3, S_4, T_C,$ and T_D are turn-on (conduction state) and remaining switches will turn-off then, the output voltage is $V_O = -V_2 = -44.5V$ at the load ends. In Mode-12, the power switches $S_2, S_4, S_5, S_A, S_B, T_C,$ and T_D are turn-on (conduction state) and remaining switches will turn-off then, the output voltage is the sum of $V_O = -(V_1 - V_2) = -89V$ at the load ends. In Mode-13, the power switches $S_2, S_4, S_A, T_C,$ and T_D are turn-on (conduction state) and remaining switches will turn-off then, the output voltage is $V_O = -V_1 = -133.5V$ at the load ends. In Mode-14, the power switches $S_3, S_4, S_A, T_C,$ and T_D are turn-on (conduction state) and remaining switches will turn-off then, the output voltage is the sum of $V_O = -(V_1 + V_2) = -178V$ at the load ends. In Mode-15, the power switches $S_1, S_2, S_5, T_C,$ and T_D are turn-on (conduction state) and remaining switches will turn-off then, the output voltage is $V_O = -V_3 = -222.5V$ at the load ends. In Mode-16, the power switches $S_1, S_3, S_5, T_C,$ and T_D are turn-on (conduction state) and remaining switches will turn-off then, the output voltage is the sum of $V_O = -(V_2 + V_3) = -267V$

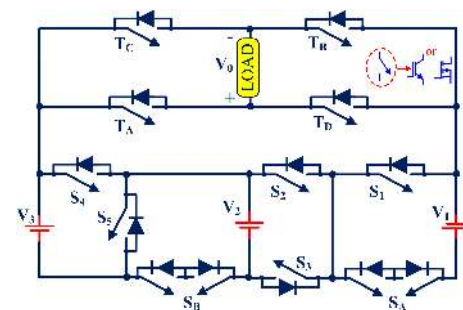


FIGURE 2. Proposed Phase Leg-A Configuration of 19MLI

at the load ends. In Mode-17, the power switches $S_2, S_A, S_B, T_C,$ and T_D are turn-on (conduction state) and remaining switches will turn-off then, the output voltage is the sum of $V_O = -(V_1 - V_2 + V_3) = -311.5V$ at the load ends. In Mode-18, the power switches $S_2, S_5, S_A, T_C,$ and T_D are turn-on (conduction state) and remaining switches will turn-off then, the output voltage is the sum of $V_O = -(V_1 + V_3) = -356V$ at the load ends. In Mode-19, the power switches $S_3, S_5, S_A, T_C,$ and T_D are turn-on (conduction state) and remaining switches will turn-off then, the output voltage is the sum of $V_O = -(V_1 + V_2 + V_3) = -400.5V$ at the load ends. The expected (typical) output and gate pulse waveform are shown in Fig.22 and simulation output voltage, current, THD, and gate pulses are generated by staircase pulse width modulation technique are shown in Fig.23 to Fig.27 respectively. The proposed 19 level asymmetrical MLI is designed in such a way that the desired output voltage to be 400V. This can be achieved by the proper design of DC sources, such as $V_1 = 133.5V, V_2 = 44.5V$ and $V_3 = 222.5V$ based on the number of levels and proposed topology. The selection of bidirectional switches at a specific location avoids the short circuit and blocks the current in both directions for a DC supply. The selected DC sources are tested with various modes of operation based on the conduction of switches regarding the switching frequency, and the expected output is achieved, which is explained in Table.1.

TABLE 1. Conduction States of Switches

L	S ₁	S ₂	S ₃	S ₄	S ₅	S _A	S _B	T _A	T _B	T _C	T _D	V _o (V)
1	0	0	1	0	1	1	0	1	1	0	0	V ₁ +V ₂ +V ₃ =400.5
2	0	1	0	0	1	1	0	1	1	0	0	V ₁ +V ₃ =356
3	0	1	0	0	0	1	1	1	1	0	0	V ₁ -V ₂ +V ₃ =311.5
4	1	0	1	0	1	0	0	1	1	0	0	V ₂ +V ₃ =267
5	1	1	0	0	1	0	0	1	1	0	0	V ₃ =222.5
6	0	0	1	1	0	1	0	1	1	0	0	V ₁ +V ₂ =178
7	0	1	0	1	0	1	0	1	1	0	0	V ₁ =133.5
8	0	1	0	1	1	1	1	1	1	0	0	V ₁ -V ₂ =89
9	1	0	1	1	0	0	0	1	1	0	0	V ₂ =44.5
10	0	0	0	0	0	0	0	1	1	0	0	0V
11	1	0	1	1	0	0	0	0	0	1	1	-V ₂ =-44.5
12	0	1	0	1	1	1	1	0	0	1	1	-(V ₁ -V ₂)=-89
13	0	1	0	1	0	1	0	0	0	1	1	-V ₁ =-133.5
14	0	0	1	1	0	1	0	0	0	1	1	-(V ₁ +V ₂)=-178
15	1	1	0	0	1	0	0	0	0	1	1	-V ₃ =-222.5
16	1	0	1	0	1	0	0	0	0	1	1	-(V ₂ +V ₃)=-267
17	0	1	0	0	0	1	1	0	0	1	1	-(V ₁ -V ₂ +V ₃)=-311.5
18	0	1	0	0	1	1	0	0	0	1	1	-(V ₂ +V ₃)=-356
19	0	0	1	0	1	1	0	0	0	1	1	-(V ₁ +V ₂ +V ₃)=-400.5

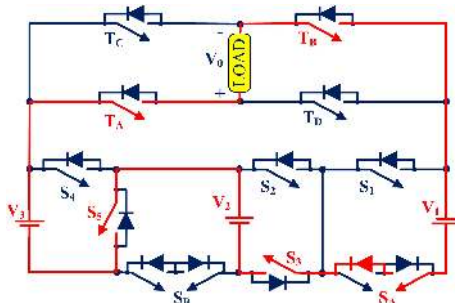


FIGURE 3. Mode-1 $V_o = V_1 + V_2 + V_3 = +400.5V$

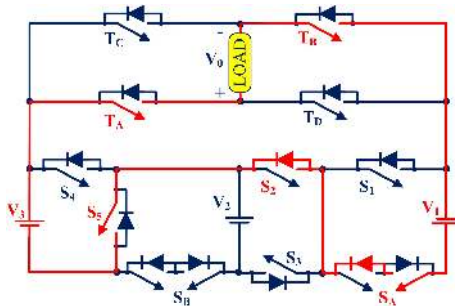


FIGURE 4. Mode-2 $V_o = V_1 + V_3 = +356V$

A. DEVELOPMENT OF POTENTIAL MLI PARAMETERS

Parameters for the proposed topology circuit are set as:
The switches number(No. of switches) are calculated as;

$$N_{switches} = 3k + 2 \quad (1)$$

If *k* is the no. of sources, then the switches no. of switches= $3 * 3 + 4 = 13$ by taking *k*=3.

The sources no. of are calculated as:

$$N_{source} = k \quad (2)$$

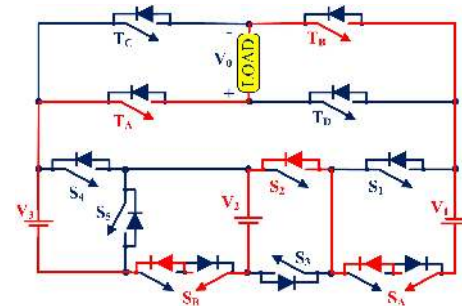


FIGURE 5. Mode-3 $V_o = V_1 - V_2 + V_3 = +311.5V$

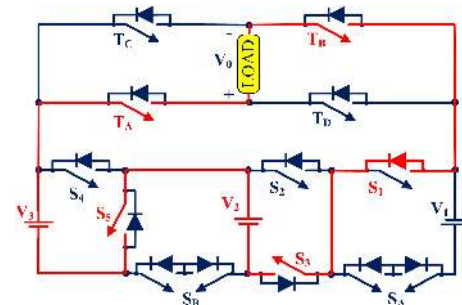


FIGURE 6. Mode-4 $V_o = V_2 + V_3 = +267V$

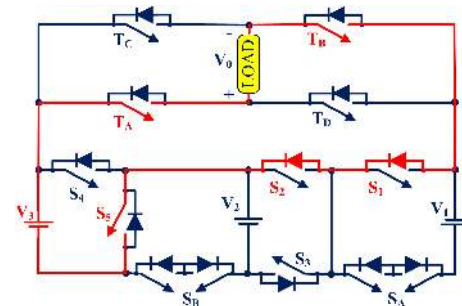


FIGURE 7. Mode-5 $V_o = V_3 = +222.5V$

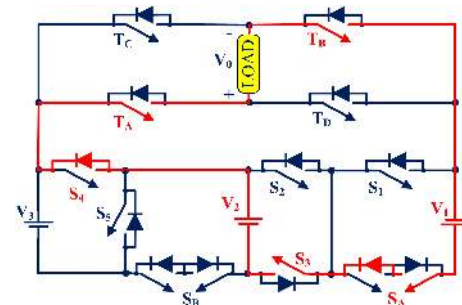


FIGURE 8. Mode-6 $V_o = V_1 + V_2 = +178V$

Then the sources are $N_{source}=3$, taking *k*=3
The output level No. of is got as;

$$N_{levels} = 2(2^k) + 3 \quad (3)$$

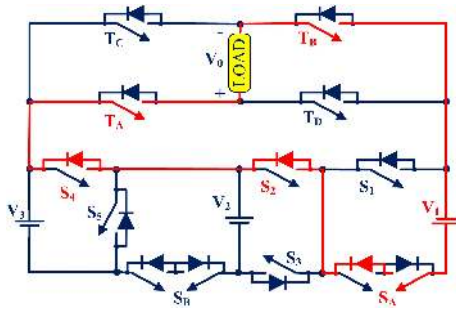


FIGURE 9. Mode-7 $V_O=V_1+V_2=133.5V$

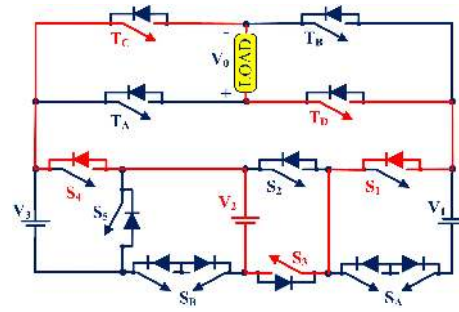


FIGURE 13. Mode-11 $V_O=-V_2=-44.5V$

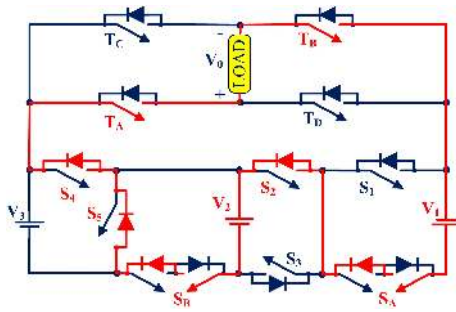


FIGURE 10. Mode-8 $V_O=V_1-V_2=89V$

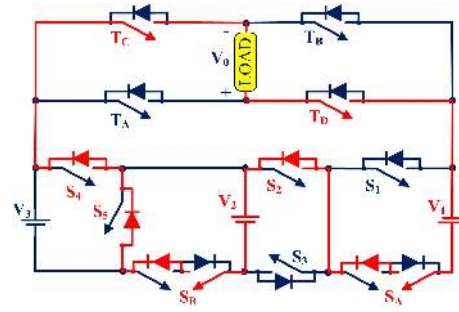


FIGURE 14. Mode-12 $V_O=-(V_1-V_2)=-89V$

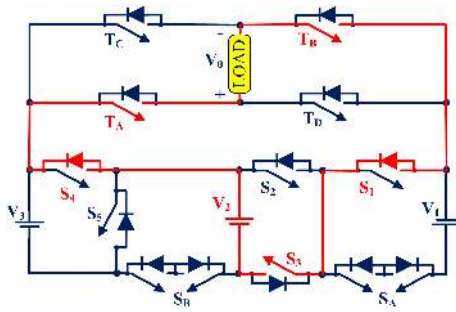


FIGURE 11. Mode-9 $V_O=V_2=44.5V$

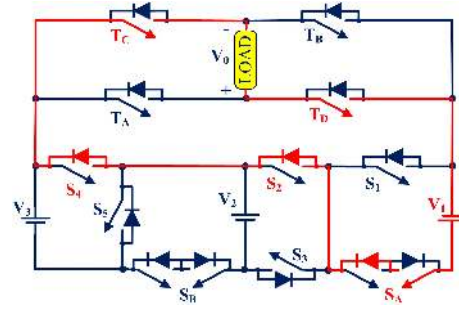


FIGURE 15. Mode-13 $V_O=-V_1=-133.5V$

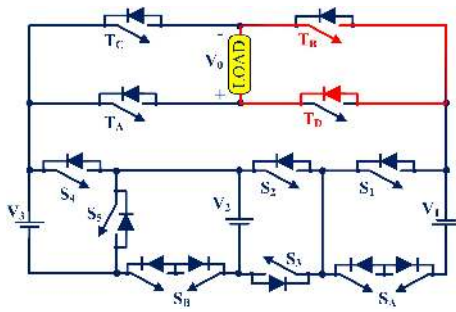


FIGURE 12. Mode-10 $V_O=0V$

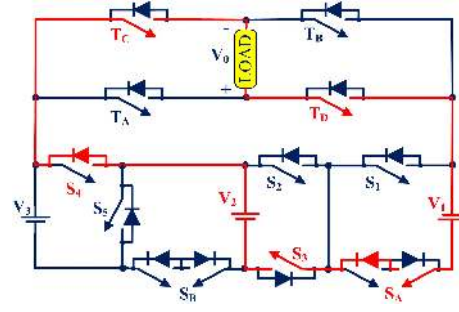


FIGURE 16. Mode-14 $V_O=-(V_1+V_2)=-178V$

Then the level no. of is $N_{level}=2(2^3 + 3) = 19$ with $k=3$
The voltage from the output is defined as;

$$V_{output} = [(2^k) + 1] * V_2 \quad (4)$$

Then the voltage of the output is
 $V_{output}=(2^3 + 1) * 44.5 = 400.5V$,
taking $k=3$ and $V_2=V_{dc}=44.5V$.

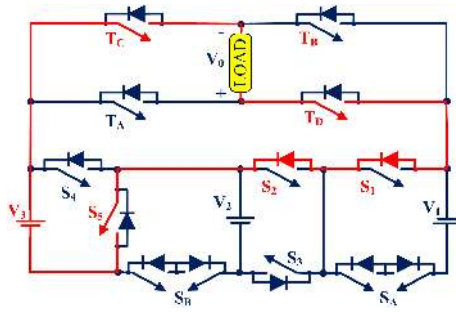


FIGURE 17. Mode-15 $V_O = -V_3 = -222.5V$

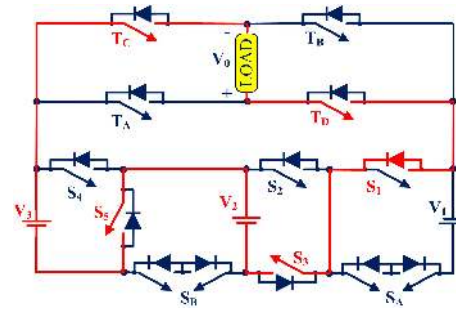


FIGURE 18. Mode-16 $V_O = -(V_2 + V_3) = -267V$

III. POWER LOSS AND EFFICIENCY CALCULATION OF MLI

The losses can be calculated in both cases, the losses of conduction and losing switching are the two key losses that follow switches. The conduction losses can be got as follows;

$$P_{Cl_IGBT(t)} = [V_{IGBT} + R_{IGBT}i^\alpha(t)] i(t) \quad (5)$$

Where V_{IGBT} is IGBT forward voltage drop, and V_d is diode drop forward voltage. The α is a constant for the IGBT specification[41, 42], and R_{IGBT} is the equivalent resistance of the IGBTs and R_d is the equivalent resistance of the diodes[41, 42]. The average value of the conductive power loss (P_{cl}) of the multilevel inverter can be given as follows[41-42], considering that the current path includes both N_{IGBT} transistor and N_d diodes at the moment t [47].

$$P_{Cl} = \frac{1}{2\pi} \int_0^{2\pi} [N_{IGBT}(t) P_{cl,IGBT}(t) dt] \quad (6)$$

Switching loss can be calculated according to the capacity used in the switches. Losses may be got depending on the turn-on and turn-off times of the switches. The losses from switching can be estimated based on linear differences in switching current and voltage. The energy figures are: Where E_{n_on} and E_{n_off} are respectively the witch k turn-ON and turn-OFF losses. The losses from switching are equal to the sum of power losses from turn-on and turn-off, calculated:

$$P_{Sl} = f \sum_{K=1}^{N_{switch}} \left[\sum_{j=1}^{N_{on,k}} E_{n_{on,kj}} + \sum_{j=1}^{N_{off,k}} E_{n_{off,kj}} \right] \quad (7)$$

The total power losses calculated as follows ($P_{total loss}$)

$$P_{total loss} = P_{cl} + P_{sl} \quad (8)$$

The efficiency of the Inverter given below

$$Efficiency = \frac{P_{out}}{P_{in}} = \frac{P_{out}}{P_{out} + P_{loss}} \quad (9)$$

Where the output power and the input power are P_{out} and P_{in} , respectively.

Can estimate the output power as follows;

$$P_{out} = V_{rms} * I_{rms} \quad (10)$$

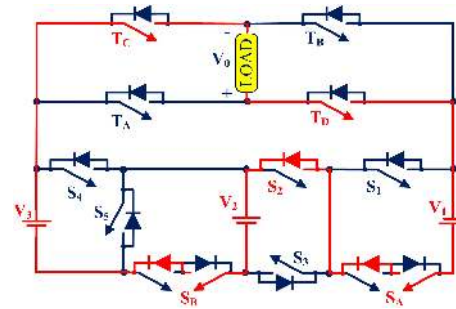


FIGURE 19. Mode-17 $V_O = -(V_1 - V_2 + V_3) = -311.5V$

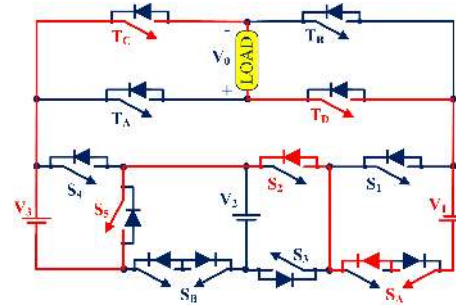


FIGURE 20. Mode-18 $V_O = -(V_1 + V_3) = -356V$

Using equation (10) ($V_{rms} = 282.4V$ & $I_{rms} = 2.828A$) the experimental output power of 799.87 W is got. For measurement, the parameter values are taken from the IGBT CM75DU-12 datasheet [41, 42]. The V_{switch} value (0.6V) is taken from the plot of performance characteristics and R_{IGBT} is 0.4-ohm, turn-on delay as 100 ns, turn-on up time as 250 ns, turn off delay time as 200 ns and turn off fall time as 300 ns for 11 switches [41, 42]. The proposed inverter architecture would require 37 measures in one full cycle. The conduction losses are determined by using equation 1; $P_{cl} = 53.854 W$, and E_{on} , E_{off} are 0.124W and 0.1625W respectively, from equation 7 the switching losses are 0.2865 W, therefore, the total losses are calculated during the conduction time and switching time by using equation 8 is 54.14W, finally from equation 9 efficiency is 93.67%.

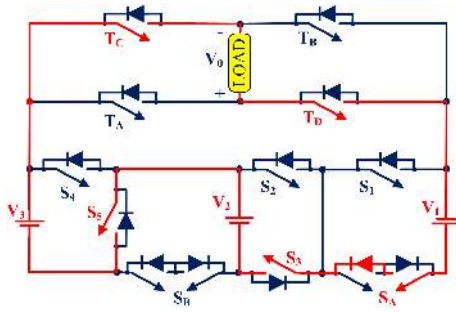


FIGURE 21. Mode-19 $V_O = -(V_1 + V_2 + V_3) = -400.5V$

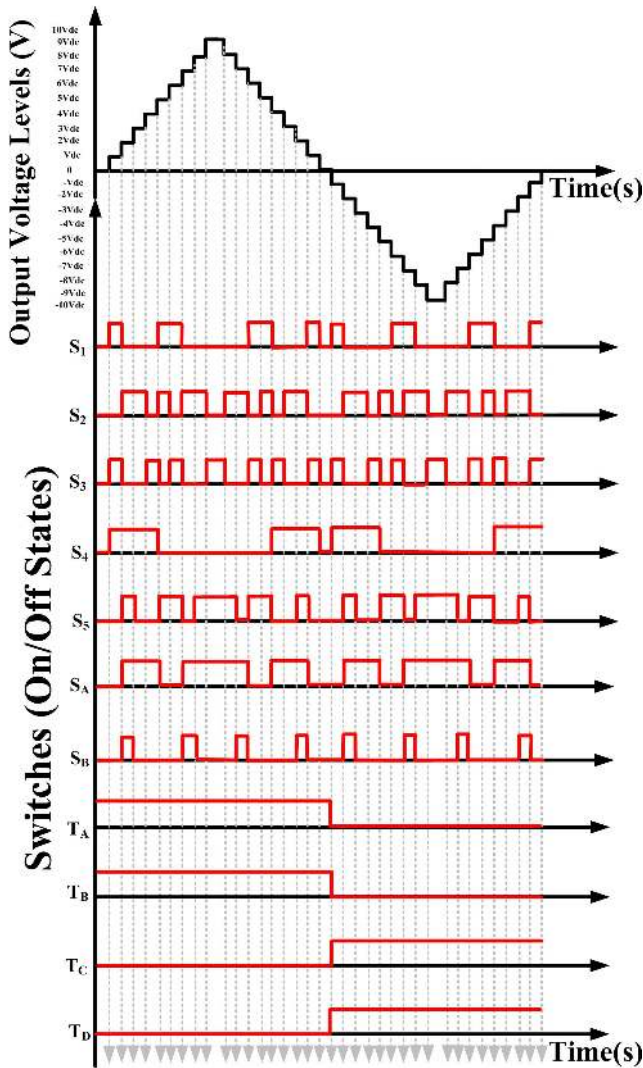


FIGURE 22. Expected (Typical) Output and Gate pulse waveform of 19 MLI

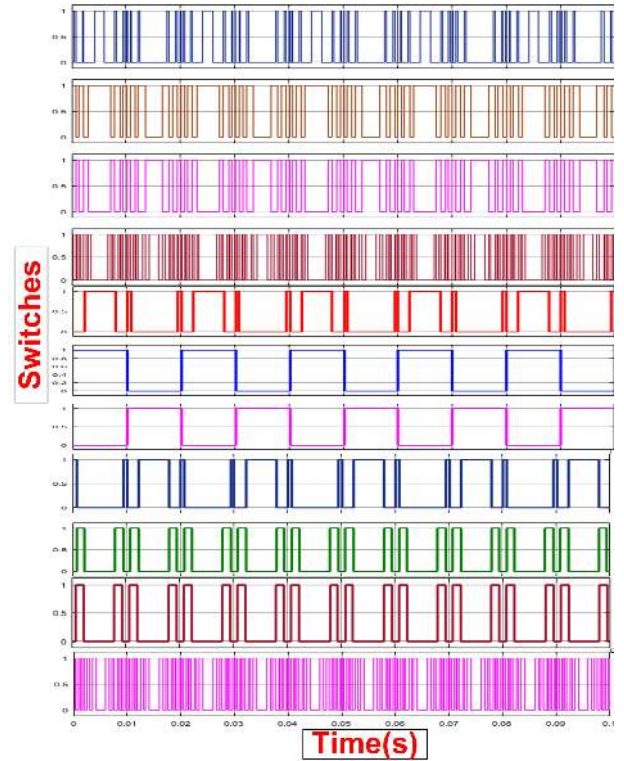


FIGURE 23. Simulation Gate pulse waveforms of 19 MLI

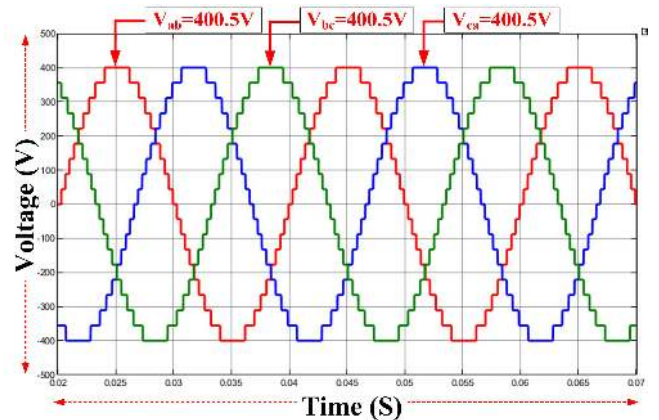


FIGURE 24. Simulation Three-Phase output waveform of 19 MLI

IV. COMPARISON WITH RECENT INVERTERS

The proposed inverter contrasted with related topologies of new inverters. Table.2 and Fig.28 to Fig.34 provides a comparison of different component parameters such as several electrical power switches (NSW), several DC sources (NDCS), driver circuits (NDC), clamping diodes (NCMP), clamping capacitors (NCP), efficiency(Eff), TSV, THD and higher output voltage levels required for the inverter proposed. thirteen power switches and three DC sources were used in this topology. Next, the sum of gate driver circuits is thus the same as the number of switches. Then, compared to existing topologies, the suggested asymmetrical topology,

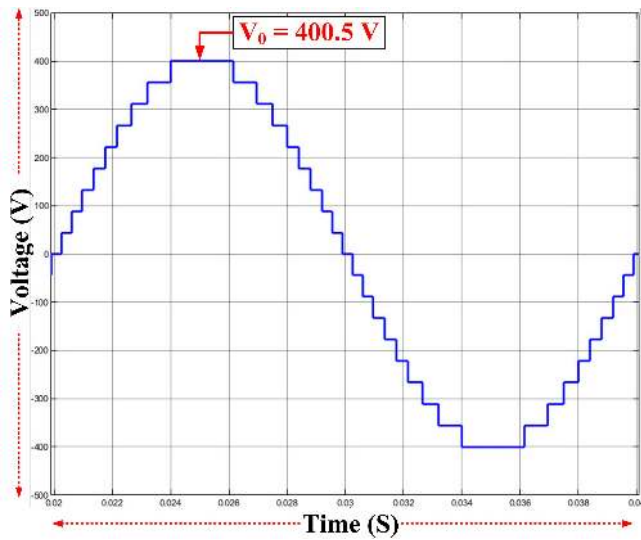


FIGURE 25. Simulation Phase Leg-A output waveform of 19 MLI

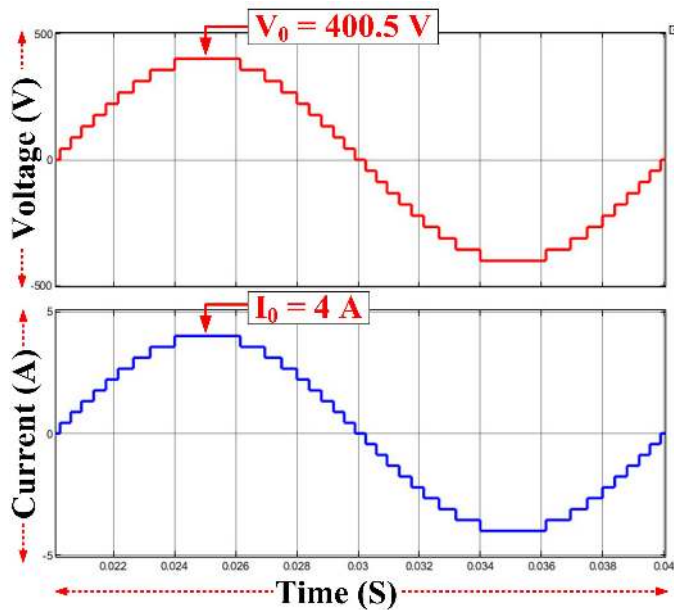


FIGURE 26. Simulation Phase Leg-A output voltage & current waveform of 19 MLI

each part was calculated for a similar voltage level. While all current topologies will need 10 to 22 switches [43-48] and 1 to 8 DC sources to provide an output voltage of 19 rates, the proposed topology needs only 13 switches and three sources with low THD. Compared with traditional topology, the drastically reduced need for switches in the proposed topology to produce better results makes it more suitable for a potential renewable application. Since the DC-link condensers are not required for the proposed topology, they are free from the question of voltage balance. Besides that, it doesn't require any capacitor clamping and diodes clamping. Every topology, therefore, has its own merits and demerits. The topology suggested has several benefits, such as fewer

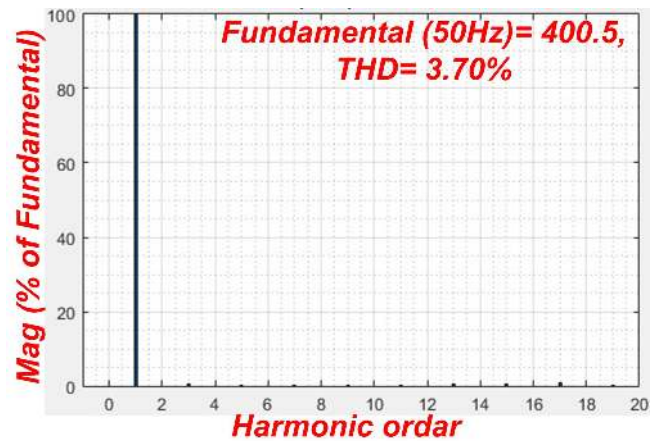


FIGURE 27. Simulation THD of 19 MLI

TABLE 2. Comparison of Proposed with Existing MLIs

Components	[43]	[44]	[45]	[46]	[47]	[48]	Proposed MLI
Switches	12	10	22	11	10	11	13
Sources	1	2	8	5	2	4	3
levels	19	19	19	19	19	19	19
Driver Circuits	11	19	22	19	10	11	13
Clamping Diodes	11	16	26	19	14	11	13
Clamping Capacitors	-	4	-	-	-	-	-
Transformers	3	-	-	-	2	-	-
%THD	-	-	3.72	3.78	3.93	-	3.89
Efficiency (%)	87.725	-	93.49	-	-	-	93.67
TSV (V)	68Vdc	80Vdc	74Vdc	72Vdc	62Vdc	52Vdc	60Vdc

switching devices, DC source count and driver circuits, and a minimum number of switches per voltage point. For asymmetric topology, the value of 3.89 percent total harmonic distortion (THD) follows the IEEE 519 requirement. Therefore, it concluded that the proposed topology requires a minimum switch count using both high and fundamental switching frequencies, thus minimizing power losses and costs.

V. TSV (TOTAL STANDING VOLTAGE) CALCULATION

The maximum voltage stress across all switches is the important parameter for the topology, and it can be represented as the total standing voltage (TSV), which is equal to the sum of maximum voltage stress across the switches [49-50]. This is an important factor for the selection of switches. Total standing voltage (TSV) is the term which is determined regarding the blocking voltages across all the switches with all voltage levels considered. The voltage stresses across each pair of the complementary switch will be same. However, the TSV is calculated for the proposed topology and is compared with various topologies and found to be the best in having the less standing voltage because of which the losses get decreased. As the blocking voltage capability is less, the rating of the switches is fewer results in cost effective. The voltage stress

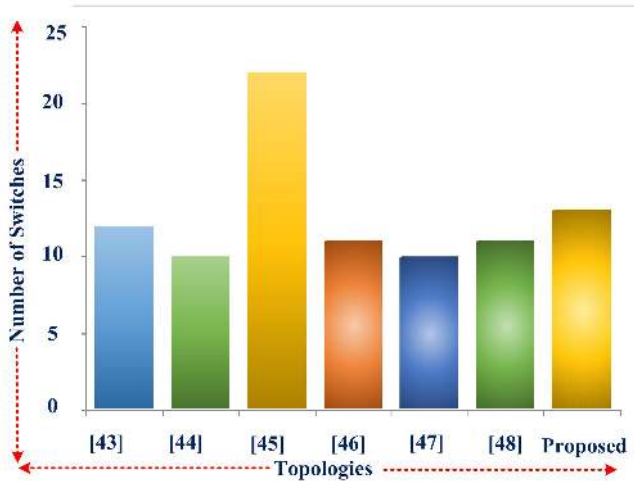


FIGURE 28. Comparison of Recent Inverters vs Proposed MLI with NWS (No. of Switches)

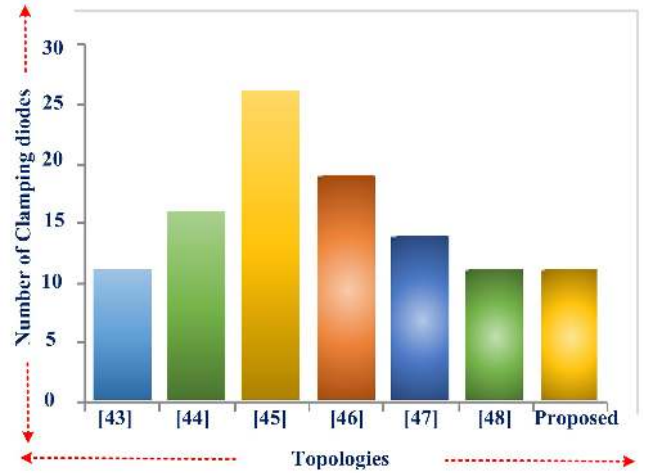


FIGURE 31. Comparison of Recent Inverters vs Proposed MLI with NCMP (No. of Clamping diodes)

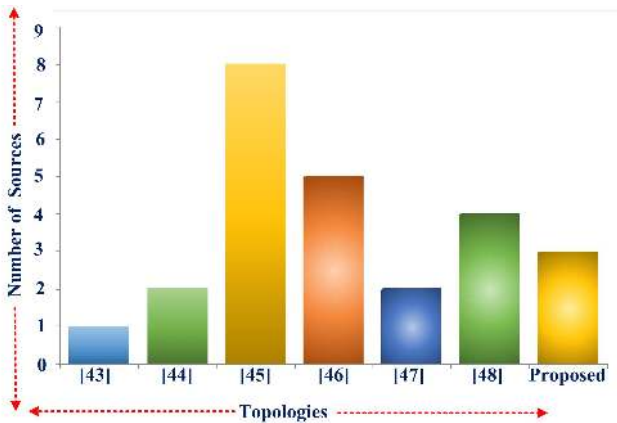


FIGURE 29. Comparison of Recent Inverters vs Proposed MLI with NDCS (No. of Sources)

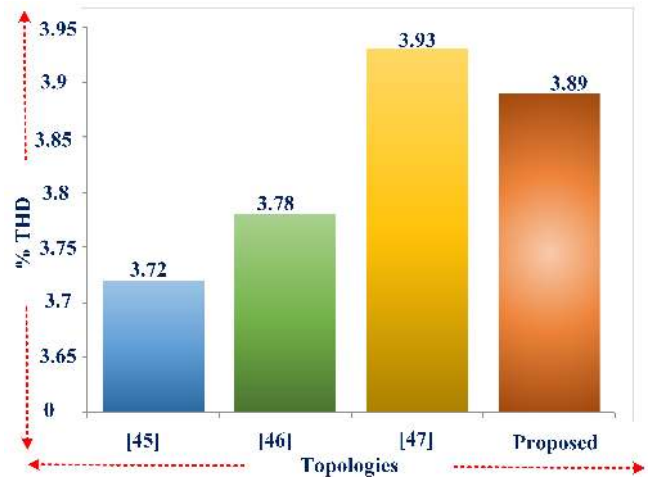


FIGURE 32. Comparison of Recent Inverters vs Proposed MLI with THD

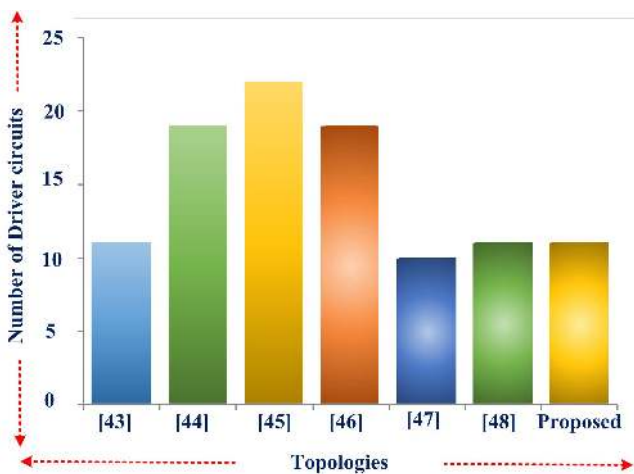


FIGURE 30. Comparison of Recent Inverters vs Proposed MLI with NDC (No. of Drivers Circuits)

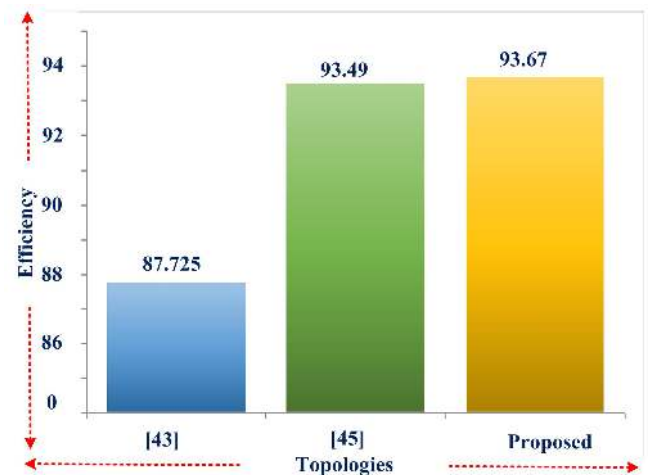


FIGURE 33. Comparison of Recent Inverters vs Proposed MLI with EFF

of the switches in different units is given as: The bidirectional switch voltages are $V_{Sbi}=V_i$ and the unidirectional switch

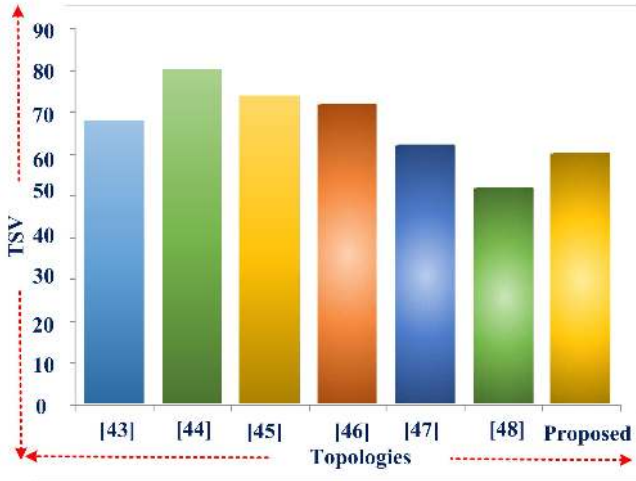


FIGURE 34. Comparison of Recent Inverters vs Proposed MLI with TSV (Total Standing Voltage)

voltages are $V_{S_{uni}}=2V_i$ where is $i =1,2,\dots,n$ and n is the number of complementary switches. With tertiary mode, the maximum output voltage ($V_{o,max}$) of the proposed topology is:

$$V_{o,max} = 400V \quad (11)$$

The total standing voltage (TSV) is an important factor for the selection of switches. TSV is the addition of the maximum blocking voltage across each semiconductor device [22]. The look-up table for 19-level inverter is shown In Table.3. Therefore, the voltage across the switches are:

$$\begin{aligned} V_{S1} &= 6V_{dc} \\ V_{S2} &= V_{S5} = 10V_{dc} \\ V_{S3} &= V_{S4} = 8V_{dc} \\ V_{TA} &= V_{TC} = 9V_{dc} \\ V_{TB} &= V_{TD} = 10V_{dc} \end{aligned}$$

The voltage stress of unidirectional switches of a bidirectional switch is given as: $V_{SA}=6V_{dc}$ and $V_{SB}=2V_{dc}$ As two unidirectional switches are used for the two bidirectional switches, blocks the voltage of 8Vdc. Therefore,

$$T_{SV} = 2(V_{S1}+V_{TD}+V_{TB})+V_{SA}+V_{SB} = 52V_{dc}+8V_{dc} = 60V_{dc} \quad (12)$$

The TSV (total standing voltages) of the proposed inverter is compared with existing inverters is shown in Fig.34.

VI. EXPERIMENTAL RESULTS

The prototype for 19 level inverter hardware setup systems is recognized and confirmed it experimentally. Fig. 44 specifies the prototype of the multilevel inverter proposed for this. Simulink block sets are dumped in to the digital I/O ports by dSPACE RTI 1104, and the MATLAB-Simulink is used to implementing the PWM form of staircase modulation (for gate pulses). Use 20 output pins, which are calculated using physical I/O ports, and real-time interfacing applications are facilitated. The pulse is created from the TLP 250 instrument, which is mined to input the RTI 1104 dSPACE. Gate driver

TABLE 3. The look up table for 19-level inverter

Level	ON Switches
1	S_3, S_5, S_A, T_A, T_B
2	S_2, S_5, S_A, T_A, T_B
3	S_2, S_A, S_B, T_A, T_B
4	S_1, S_3, S_5, T_A, T_B
5	S_1, S_2, S_5, T_A, T_B
6	S_3, S_4, S_A, T_A, T_B
7	S_2, S_4, S_A, T_A, T_B
8	$S_2, S_4, S_5, S_A, S_B, T_A, T_B$
9	S_1, S_3, S_4, T_B, T_D
10	$T_A, T_B,$
11	S_1, S_3, S_4, T_C, T_D
12	$S_2, S_4, S_5, S_A, S_B, T_C, T_D$
13	S_2, S_4, S_A, T_C, T_D
14	S_3, S_4, S_A, T_C, T_D
15	S_1, S_2, S_5, T_C, T_D
16	S_1, S_2, S_3, T_C, T_D
17	S_2, S_A, S_B, T_C, T_D
18	S_2, S_5, S_A, T_C, T_D
19	S_3, S_5, S_A, T_C, T_D

is used to boosting the 5 V to 15 V PWM pulse setup. The control switch is turned on with a 15V pulse. The specifications of the prototype model part are shown in Table 5, the results of the prototype investigation are verified at a steady-state, load disturbance situations are conducted with the help of resistive, inductive loads, and THD is shown in Figures 35 to 43, respectively. The pulses from the gate produced using Driver Circuit TLP250 is shown in Figure.35. The steady-state study was verified with 400 V resistive load (R load), with 4 A attaining output current. The RMS output and voltage found at 282.84 V and 2.828 A current, respectively. The hardware tests are shown respectively in Figure.36, Figure.37, Figure.38 and Figure.39. The experimental prototype results show notably that with 19 output voltage levels. Speciously, the waveform shows that the angle of the transition between the charge current and the charge voltage is zero. After the achievements of steady-state testing with resistive load, we presented 400 V motor (inductive value is 98mH with 50ohm internal resistance) load (loading power factor) and 6.8 A current. The output current and voltage RMS value are respectively reached with 282.84 V and current 4.808 A. The experimental findings are given in Figure.40. The results show that, with 19 output voltage levels. The phase angle between the lagging charge current and the lagging load voltage is shown in the waveform. To be sure, tons rarely happen distinctly. These can happen continuously in resistive and inductive loads. Typically, where a resistive load is present, an unforeseen addition of inductive load is likely to match the resistive load in parallel or vice versa. The output voltage must stay steady even in these circumstances is shown in Figure.41 and Figure.42. Figure 39, and Figure 40 shows the experimental voltage THD is 3.89 percent. The experimental component requirements are tabled in Table.5. The proposed MLI could produce higher voltage outputs with fewer hardware components and low THD. The proposed 19 MLI is tested experimentally

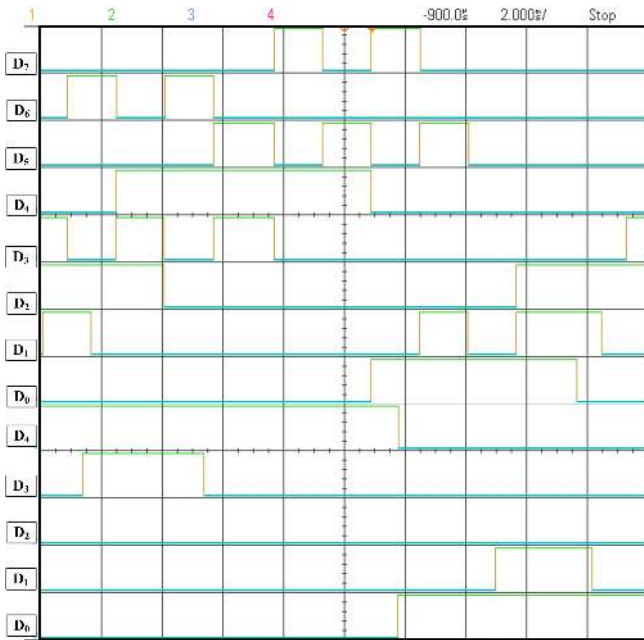


FIGURE 35. Experimental Gates Pulses of 19 MLI

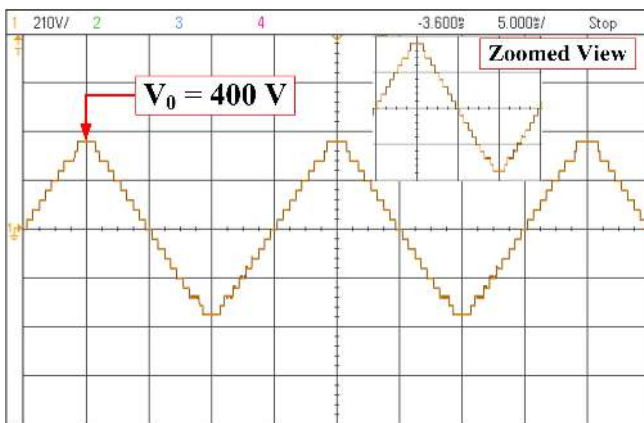


FIGURE 36. Experimental Output waveform of Phase Leg-A 19 MLI

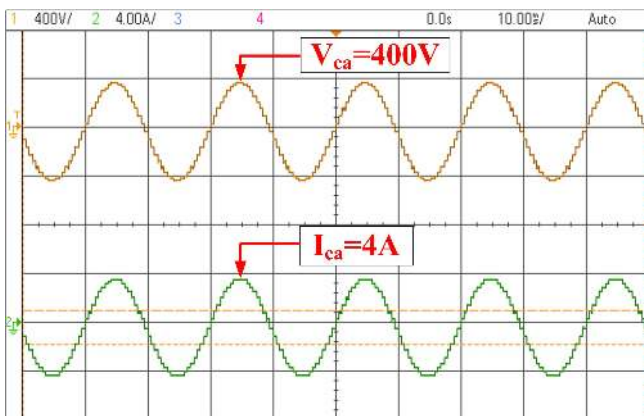


FIGURE 37. Experimental Output voltage & current waveform of 19 MLI

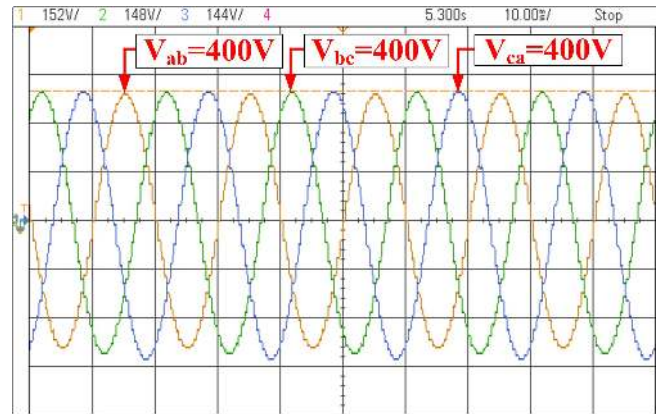


FIGURE 38. Experimental Output waveform of Three-Phase 19 MLI

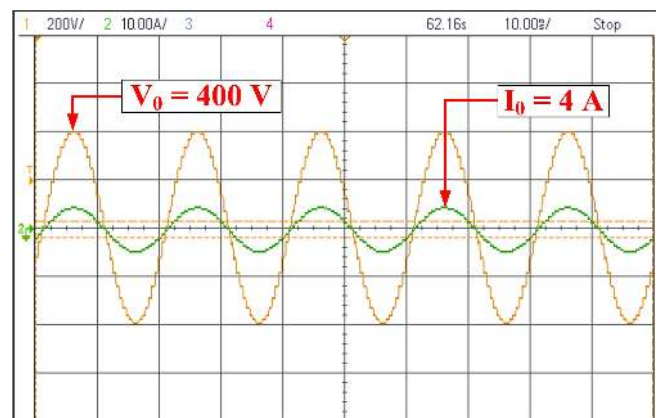


FIGURE 39. Experimental Output waveform of Phase Leg-A with R Load

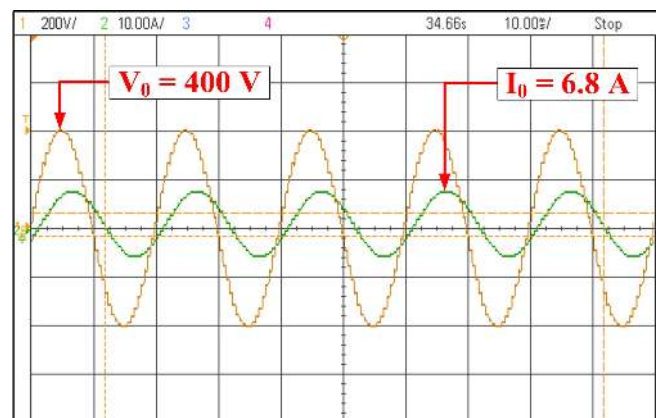


FIGURE 40. Experimental Output waveform of Phase Leg-A with L (Motor) Load

with L (motor), RL and LR loads. The results got are like simulation. The three-phase line to line voltage of simulation is 400.5 V whereas 400V got experimentally in all phases shown in Table.4. The phase leg-A with equal magnitude are 400V, 4A in both simulation and experimental results. The output waveform of phase leg-A is tested with R, motor, RL and LR loads: with R load, 400V, 4A and 798.62W are

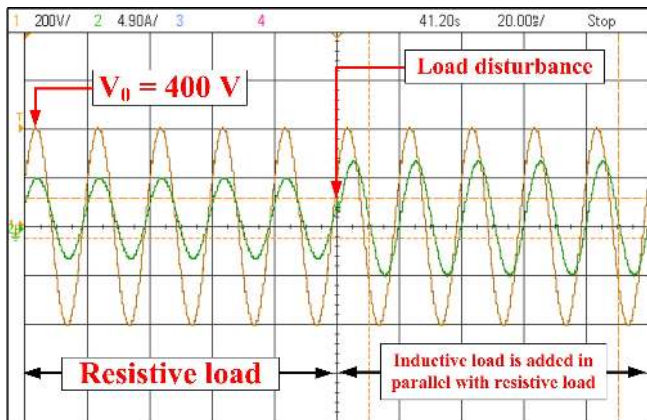


FIGURE 41. Experimental Output waveform of Phase Leg-A with RL Load

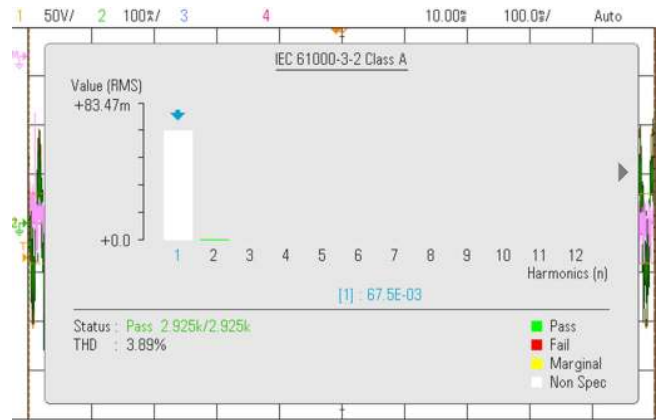


FIGURE 43. Experimental THD of 19MLI

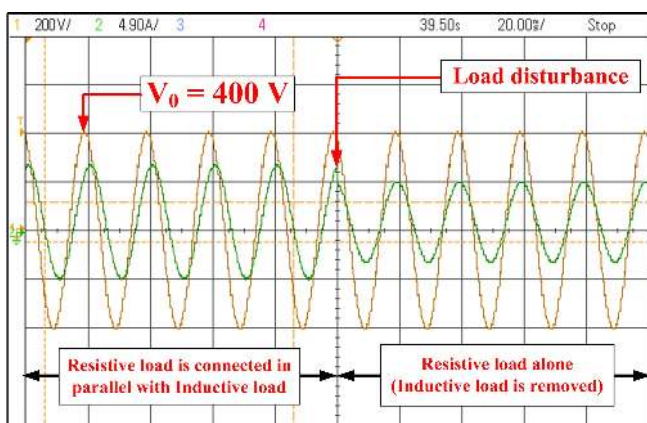


FIGURE 42. Experimental Output waveform of Phase Leg-A with LR Load

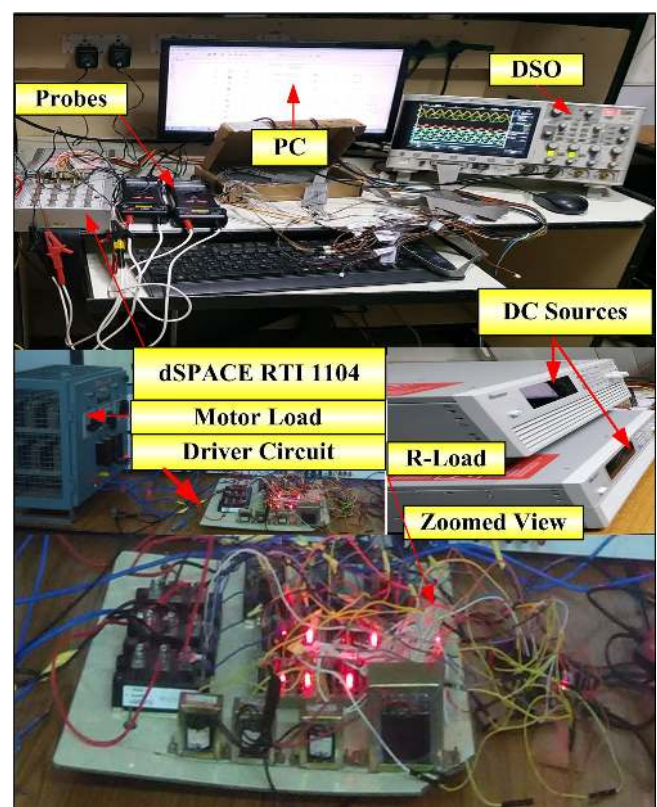


FIGURE 44. Prototype Model of 19MLI

got at output, with L (motor) load, 400V and 6.8A are got, In RL load, 400V remains in both resistive and inductive operation resembling the systems output is stable, during load disturbance R and L are in parallel. In LR load, 400V remains in both inductive and resistive operation resembling the stable output, and during the load disturbance, resistive load is alone in the system. THD in simulation is 3.7% whereas 3.89% experimentally. The proposed inverter is designed with optimal hardware components with improved efficiency, reduced power losses, lower THD compared to existing MLIs. The proposed inverter well suits for renewable energy applications.

TABLE 4. Simulation and experimental results

19 MLI output parameters	Simulation	Experimental
Three phase line to line output voltage	400.5V per phase	400V per phase
Phase leg-A (Line to Line)	400.5V, 4A	400V, 4A
Phase leg-A (Equal magnitude)	400V	400V, 4A
R-Load	400V, 4A	400V, 4A
RMS Voltage and Current	282.4V, 2.828A	282.4V, 2.828A
L-Load (Motor)	400V	400V, 6.8A
THD %	3.7%	3.89%

TABLE 5. Experimental Specification

Component	Type	ratings
Switches	IGBT-CM75DU-12H	600V,75A
Driver ICs	TLP250	-
Power supply	Programmable DC Sources	0-500V
Controller	dSPACE	RTI1104
Load	Resistive and Motor (Inductor)	100 ohm and 98mH

VII. CONCLUSION

A three-phase nineteen level asymmetric MLI is tested and implemented. The proposed inverter generates an increased number of output voltage levels with a lesser amount of DC sources and power switches. This inverter makes a voltage at 3.89 % THD, and efficiency is 93.67% got according to IEEE standards. The proposed inverter is tested with study-sate and dynamic load disturbance. In this paper, a reduced part count of 19-level inverter topology proposed for high-reliability renewable energy applications. The proposed topology used the inherent properties of sinusoidal voltages to minimize part count to improve the efficiency of the inverter without the sizing of the circuit components. The proposed inverter balanced well during complex charging (load disturbance) conditions. This inverter is highly adaptive for high-power and renewable energy systems.

REFERENCES

- [1] Nabae, Akira and Takahashi, Isao and Akagi, Hirofumi, "A new neutral-point-clamped PWM inverter," *IEEE Transactions on industry applications*, no.5, pp. 518–523, 1986.
- [2] Rodriguez, Jose and Lai, Jih-Sheng and Peng, Fang Zheng, "Multilevel inverters: a survey of topologies, controls, and applications," *IEEE Transactions on industrial electronics*, vol. 49, no.4, pp. 724–738, Aug. 2002.
- [3] Lai, Y-S and Shyu, F-S "Topology for hybrid multilevel inverter," *IEE Proceedings-Electric Power Applications*, vol. 149, no.6, pp. 449–458, 2002.
- [4] Meynard, TA and Foch, H, "Multi-level choppers for high voltage applications," *EPE journal*, vol. 2, no.1, pp. 45–50, 1992.
- [5] Mueller, O. M., and J. N. Park, "Quasi-linear IGBT inverter topologies," *Proceedings of 1994 IEEE Applied Power Electronics Conference and Exposition-ASPEC'94*, IEEE, 1994.
- [6] Manjrekar, Madhav D., Peter K. Steimer, and Thomas A. Lipo, "Hybrid multilevel power conversion system: A competitive solution for high-power applications," *IEEE Transactions on industry applications*, vol. 36, no.3, pp. 834–841, 2000.
- [7] Baker, Richard H, "High-voltage converter circuit." *US Patent 4,203,151*, pp.151-123, 1980.
- [8] Ahmed, Mahrous E and Mekhilef, Saad, "Design and implementation of a multi level three-phase inverter with less switches and low output voltage distortion," *Journal of Power Electronics*, vol. 9, no.4, pp. 593–603, 2009.
- [9] Optimized modulation techniques for the generalized N-level converter, "Optimized modulation techniques for the generalized N-level converter," *PESC'92 Record. 23rd Annual IEEE Power Electronics Specialists Conference*, pp. 1205–1213, 1992.
- [10] Meynard, TA and Foch, Henry, "Multi-level conversion: high voltage choppers and voltage-source inverters," *PESC'92 Record. 23rd Annual IEEE Power Electronics Specialists Conference*, pp. 397–403, 1992.
- [11] Marquardt, R. "A new modular voltage source inverter topology." *Conf. Rec. EPE 2003*, 2003.
- [12] Lesnicar, Anton, and Rainer Marquardt. "An innovative modular multilevel converter topology suitable for a wide power range." *2003 IEEE Bologna Power Tech Conference Proceedings*, Vol. 3. IEEE, 2003.
- [13] Yuan, Xiaoming, and Ivo Barbi. "Fundamentals of a new diode clamping multilevel inverter." *IEEE Transactions on power electronics* 15.4, 711–718, 2000.
- [14] Kadir, MN Abdul, Saad Mekhilef, and Hew Wooi Ping. "Dual vector control strategy for a three-stage hybrid cascaded multilevel inverter." *Journal of Power Electronics*, pp. 155-164, 2010.
- [15] Huang, Jing, and Keith A. Corzine. "Extended operation of flying capacitor multilevel inverters." *IEEE transactions on power electronics* 21.1, pp. 140-147, 2006.
- [16] Feng, Chunmei, Jun Liang, and Vassilios G. Agelidis. "Modified phase-shifted PWM control for flying capacitor multilevel converters." *IEEE Transactions on Power Electronics*, 22(1), pp. 178-185, 2007.
- [17] Banaei, M. R., A. R. Dehghanzadeh, Ebrahim Salary, Hossein Khounejahan, and Rana Alizadeh, "Z-source-based multilevel inverter with reduction of switches." *IET power electronics*, 5(3), pp. 385-392, 2012.
- [18] Kangarlu, M. Farhadi, E. Babaei, and Sara Laali, "Symmetric multilevel inverter with reduced components based on non-insulated dc voltage sources." *IET Power Electronics*, 5(5) pp. 571-581, 2012.
- [19] Babaei, Ebrahim. "A cascade multilevel converter topology with reduced number of switches." *IEEE Transactions on power electronics*, 23(6), pp. 2657-2664, 2008.
- [20] Waltrich, Gierry, and Ivo Barbi. "Three-phase cascaded multilevel inverter using power cells with two inverter legs in series." *2009 IEEE Energy Conversion Congress and Exposition*, 2009.
- [21] Dixon, Juan, and Luis Moran. "High-level multistep inverter optimization using a minimum number of power transistors." *IEEE transactions on power electronics*, 21(2) pp. 330-337, 2006.
- [22] Siddique, Marif Daula, Saad Mekhilef, Noraisyah Mohamed Shah, Adil Sarwar, Atif Iqbal, and Mudasir Ahmed Memon, "A New Multilevel Inverter Topology With Reduce Switch Count" *IEEE Access*, vol. 7, pp. 58584-58594,2019, doi: 10.1109/ACCESS.2019.2914430.
- [23] Rufer, A and Veenstra, M and Gopakumar, K, "Asymmetric multilevel converter for high resolution voltage phasor generation," *Proc. EPE*, pp. 0-10, 1999.
- [24] Veenstra, Martin and Rufer, Alfred, "Control of a hybrid asymmetric multilevel inverter for competitive medium-voltage industrial drives," *IEEE Transactions on industry applications*, vol.41 no.2, pp. 655–664, 2005.
- [25] Mekhilef, Saad and Omar, AM and Rahim, NA, "Modelling of three-phase uniform symmetrical sampling digital PWM for power converter," *Canadian Conference on Electrical and Computer Engineering*, 2005, pp. 1505–1508, 2008.
- [26] Mariethoz, SAlbastien, and Alfred Rufer, "Design and control of asymmetrical multi-level inverters," *IEEE 2002 28th Annual Conference of the Industrial Electronics Society. IECON 02*, pp. 840–845, 2002.
- [27] Blaabjerg, Frede, Zhe Chen, and Soeren Baekhoej Kjaer, "Power electronics as efficient interface in dispersed power generation systems," *IEEE transactions on power electronics*, vol. 9, no.5, pp. 1184–1194, 2004.
- [28] Rajkumar, M Valan and Manoharan, PS, "Modeling and Simulation of Five-level Five-phase Voltage Source Inverter for Photovoltaic Systems," *Journal Przeglad Elektrotechniczny*, vol. 10, no.10, pp. 237–241, 2013.
- [29] Selvakumar, S and Vinothkumar, A and Vigneshkumar, M, "An efficient new hybrid cascaded H-bridge inverter for photovoltaic system," *2014 2nd International Conference on Devices, Circuits and Systems (ICDCS)*, pp.1–6, 2006.
- [30] Babaei, Ebrahim and Sara laali, "New extendable 15-level basic unit for multilevel inverters," *Journal of Circuits, Systems and Computers*, vol. 25, no.12, pp. 1650151, 2016.
- [31] Ahmed, Rokan Ali, Saad Mekhilef, and Hew Wooi Ping, "New multilevel inverter topology with minimum number of switches," *TENCON 2010-2010 IEEE Region 10 Conference*, pp. 1862–1867, 2010.
- [32] Vijayaraja, L., S. Ganesh Kumar, and M. Rivera, "A New Topology of Multilevel Inverter with reduced part count" *2018 IEEE International Conference on Automation/XXIII Congress of the Chilean Association of Automatic Control (ICA-ACCA)*, pp. 1–5, 2018.
- [33] Dahidah, Mohamed SA, Georgios S. Konstantinou, and Vassilios G. Agelidis, "SHE-PWM control for asymmetrical hybrid multilevel flying capacitor and H-bridge converter" *2011 IEEE Ninth International Conference on Power Electronics and Drive Systems*, pp. 29–34, 2011.
- [34] Babaei, Ebrahim, "Charge balance control methods for a class of fundamental frequency modulated asymmetric cascaded multilevel inverters," *Journal of Power Electronics*, vol. 11, no.6, pp.811–818, 2011.
- [35] Bircenas, E., Sinuhe Ramirez, Victor Cardenas, and R. Echavarria, "Cascade multilevel inverter with only one DC source", *VIII IEEE International Power Electronics Congress, 2002. Technical Proceedings. CIEP 2002*, pp. 171–176, 2002.
- [36] Sabahi, M., AR Marami Iranqa, K. Mehdi Bahrami, K. Mojtaba Bahrami, and M. B. B. Sharifian. "Harmonics elimination in a multilevel inverter with unequal DC sources using genetic algorithm." *2011 International Conference on Electrical Machines and Systems*, IEEE, 2011.
- [37] Lin, Bor-Ren, Ta-Chang Wei, and Huann-Keng Chiang. "An eight-switch three-phase VSI for power factor regulated shunt active filter," *Journal of Power Electronics*, vol. 68, no.2, pp. 157–165, 2004.
- [38] Nami, Alireza, Firuz Zare, Arindam Ghosh, and Frede Blaabjerg. "A hybrid cascade converter topology with series-connected symmetrical and asymmetrical diode-clamped H-bridge cells." *IEEE transactions on power electronics* vol. 26 no.1, pp. 51-65, 2009.
- [39] Dhanamjayulu, C and Meikandasivam, S, "Implementation and comparison of symmetric and asymmetric multilevel inverters for dynamic loads," *IEEE Access*, vol. 6, pp. 738–746, 2017.

- [40] Dhanamjayulu, C and Meikandasivam, S, "Design and implementation of symmetric cascaded multilevel inverter using sub multi-cells," *Journal of Advanced Research in Dynamical and Control Systems*, vol. 9, no.18, pp. 1657-1668, 2017.
- [41] Dhanamjayulu, C., G. Arunkumar, B. Jaganatha Pandian, CV Ravi Kumar, M. Praveen Kumar, A. Rini Ann Jerin, and P. Venugopal. "Real-time implementation of a 31-level asymmetrical cascaded multilevel inverter for dynamic loads," *IEEE Access*, vol. 7, pp. 51254–51266, 2019.
- [42] Dhanamjayulu, Chittathuru, Gopal Arunkumar, Balakrishnan Jaganatha Pandian, and Sanjeevikumar Padmanaban. "Design and implementation of a novel asymmetrical multilevel inverter optimal hardware components," *International Transactions on Electrical Energy Systems*, vol. 30, no.2, pp. 1-28, 2020.
- [43] Kang, Feel-soon, "A modified cascade transformer-based multilevel inverter and its efficient switching function," *Electric Power Systems Research*, vol. 79, no.12, pp. 1648–1654, 2009.
- [44] Barzegarkhoo, Reza, Elyas Zamiri, Majid Moradzadeh, and Hamed Shadabi. "Symmetric hybridised design for a novel step-up 19-level inverter." *IET Power Electronics*, vol. 10, no.11, 1377-1391, 2017.
- [45] Tsang, Kai-Ming and Chan, Wai-Lok, "Single DC source three-phase multilevel inverter using reduced number of switches," *IET Power Electronics*, vol. 7, no.4, pp. 775–783, 2013.
- [46] Alishah, Rasoul Shalchi, et al. "New hybrid structure for multilevel inverter with fewer number of components for high-voltage levels." *IET power electronics*, vol. 7, no.1, 96-104, 2014.
- [47] Venkataramanaiah, J and Suresh, Y and Panda, Anup Kumar, "Design and development of a novel 19-level inverter using an effective fundamental switching strategy," *IEEE Journal of Emerging and Selected Topics in Power Electronics*, vol. 6, no.4, pp. 1903–1911, 2017.
- [48] Babaei, Ebrahim and Dehqan, Ali and Sabahi, Mehran, "A new topology for multilevel inverter considering its optimal structures," *Electric Power Systems Research*, vol. 103, pp. 145–156, 2013.
- [49] Siddique, Marif Daula, Atif Iqbal, Mudasir Ahmed Memon, and Saad Mekhilef. "A New Configurable Topology for Multilevel Inverter With Reduced Switching Components," *IEEE Access*, vol. 8, pp. 188726-188741, 2020.
- [50] Siddique, Marif Daula, Saad Mekhilef, Noraisyah Mohamed Shah, Jagabar Sathik Mohamed Ali, Mehdi Seyedmahmoudian, Ben Horan, and Alex Stojcevski. "Switched-capacitor-based boost multilevel inverter topology with higher voltage gain" *IET Power Electronics*, vol. 13.14, pp. 3209-3212, 2020.



DHANAMJAYULU C (Member, IEEE) received the B.Tech. degree in electronics and communication engineering from JNTU University, Hyderabad, India, the M.Tech. degree in control and instrumentation systems from Indian Institute of Technology Madras, Chennai, India, and the Ph.D. degree in power electronics from the Vellore Institute of Technology, Vellore, India. He is currently a Postdoctoral Researcher with the Department of Energy Technology, Aalborg University, Esbjerg,

Denmark. He is currently a Faculty Member and a member of the Control and Automation Department, School of Electrical Engineering, Vellore Institute of Technology. He is also a Senior Assistant Professor with the School of Electrical Engineering, Vellore Institute of Technology. Since 2010, he has been a Senior Assistant Professor with the Vellore Institute of Technology. He was invited as a Visiting Researcher with the Department of Energy Technology, Aalborg University, Esbjerg, Denmark, funded by the Danida Mobility Grant, Ministry of Foreign Affairs of Denmark on Denmark's International Development Cooperation. His research interests include multilevel inverters, power converters, active power filters, power quality, grid-connected systems, smart grid, electric vehicle, electric spring, and tuning of memory elements and controller parameters using soft-switching techniques for power converters, average modeling, steady-state modeling, small-signal modeling stability analysis of the converters and inverters.



PALANISAMY KALIANNAN (M'07–SM'18) received the bachelor's degree in electrical engineering from the KSR College of Technology, India, in 2000, the master's (Hons.) degree in Applied Electronics from the Coimbatore Institute of Technology, India, in 2004, and the Ph.D. degree in electrical engineering from Vellore Institute of Technology, Vellore, India, in 2013. He is currently an Deputy Director-Electrical Maintenance and Projects, Associate Professor of Energy and

Power Electronics Division and head of center for smart grid technology at Vellore Institute of Technology between 2007 to till date. From 2016 to 2018 he was a head of the department Energy and Power Electronics Division. He has authored over 96 scientific papers in referred conference proceedings and international journals in the field of renewable energy, battery energy storage, multilevel converters and power quality. He is a certified Energy Auditor by the Bureau of Energy Efficiency, Government of India. He has taken up various consultancy projects in energy efficiency and power quality improvement.



SANJEEVIKUMAR PADMANABAN (M'12–SM'15) received the bachelor's degree in electrical engineering from the University of Madras, Chennai, India, in 2002, the master's degree (Hons.) in electrical engineering from Pondicherry University, Puducherry, India, in 2006, and the PhD degree in electrical engineering from the University of Bologna, Bologna, Italy, in 2012. He was an Associate Professor with VIT University from 2012 to 2013. In 2013, he joined the National

Institute of Technology, India, as a Faculty Member. In 2014, he was invited as a Visiting Researcher at the Department of Electrical Engineering, Qatar University, Doha, Qatar, funded by the Qatar National Research Foundation (Government of Qatar). He continued his research activities with the Dublin Institute of Technology, Dublin, Ireland, in 2014. Further, he served an Associate Professor with the Department of Electrical and Electronics Engineering, University of Johannesburg, Johannesburg, South Africa, from 2016 to 2018. Since 2018, he has been a Faculty Member with the Department of Energy Technology, Aalborg University, Esbjerg, Denmark. He has authored over 300 scientific papers.

S. Padmanaban was the recipient of the Best Paper cum Most Excellence Research Paper Award from IET-SEISCON'13, IET-CEAT'16, IEEE-EECSI'19, IEEE-CENCON'19 and five best paper awards from ETAERE'16 sponsored Lecture Notes in Electrical Engineering, Springer book. He is a Fellow of the Institution of Engineers, India, the Institution of Electronics and Telecommunication Engineers, India, and the Institution of Engineering and Technology, U.K. He is an Editor/Associate Editor/Editorial Board for refereed journals, in particular the IEEE SYSTEMS JOURNAL, IEEE Transaction on Industry Applications, IEEE ACCESS, IET Power Electronics, IET Electronics Letters, and Wiley-International Transactions on Electrical Energy Systems, Subject Editorial Board Member Energy Sources Energies Journal, MDPI, and the Subject Editor for the IET Renewable Power Generation, IET Generation, Transmission and Distribution, and FACTS journal (Canada).



PANDAV KIRAN MAROTI (S'17–M'19) received the Bachelor Degree in Electronics and Telecommunication from Dr. Babasaheb Ambedkar Marathwada University, Aurangabad (India) in 2011, Master of Technology in Power Electronics and Drives with distinction from Vellore Institute of Technology, Vellore (India) in 2014. He is perusing Ph.D. degree in the field of Power Electronics at University of Johannesburg, South Africa and also received GLOBAL

EXPERIENCE SCHOLARSHIP (GES). Now he is a Visiting Researcher at Qatar University. He was working as Assistant Professor in Marathwada Institute of Technology, Aurangabad, Maharashtra (India) from 2014 to 2016. He has published scientific papers in the field of Power Electronics (Multilevel DC/DC and DC/AC converter, multiphase open winding inverter). He received the best paper award from ETAERE in 2016 sponsored Lecture note in Electrical Engineering, Springer book series. He is an active professional member of IEEE, Industrial Electronics, Power Electronics, Industrial Application, and Young Professionals societies. Also, he is an active reviewer member of various reputed international conferences and journal including IEEE and IET.



DR JENS BO HOLM-NIELSEN, Born 1954; PhD. Head of the Research Group of Bioenergy and Green Engineering, Department of Energy Technology, Aalborg University, Denmark. 30 years of experience in the field of Biomass feedstock production, Biorefinery concepts and Biogas production. Board member of R & D, committees of the cross-governmental body of biogas developments 1993-2009, Denmark. Secretary and/or chair of NGO biogas and bioenergy organizations.

Chair and presenter of Sustainable and 100 per cent Renewables and SDG-17 goals. Experience of a variety of EU projects, organizer of international conferences, workshops and training programs in EU, USA, Canada, China, Brazil, India, Iran, Russia, Ukraine, among others. Research: Managing research, development and demonstration programs in Integrated agriculture, environment and energy systems. Fulfilled the biomass and bio-energy R & D projects. His principle focuses on biofuels, biogas and biomass resources. EDU and Supervising M.Sc. and PhD students in these research fields. Training programs: International courses, training programs, and supervision for PhD students and academic staff, governmental bodies and experts in bioenergy systems. His full biography at www.aau.dk profile search Jens Bo Holm-Nielsen.

• • •